行政院國家科學委員會補助專題研究計畫 ■ 成 果 報 告 □期中進度報告

計畫名稱： 粒狀磁性固體與薄膜晶粒邊界穿隧方式磁阻機制之比較研究

計畫類別：■個別型計畫　　□ 整合型計畫
計畫編號：NSC 94－2112－M－164－001－
執行期間：94 年 08 月 01 日至 95 年 07 月 31 日

計畫主持人：楊尚霖教授兼系主任
共同主持人：
計畫參與人員：謝承達，林宸澂，林昆鴻，施旻吾

成果報告類型(依經費核定清單規定繳交)：■精簡報告　□完整報告

本成果報告包括以下應繳交之附件：
□赴國外出差或研習心得報告一份
□赴大陸地區出差或研習心得報告一份
■出席國際學術會議心得報告及發表之論文各一份
□國際合作研究計畫國外研究報告書一份

處理方式：除產學合作研究計畫、提升產業技術及人才培育研究計畫、列管計畫及下列情形者外，得立即公開查詢
□ 涉及專利或其他智慧財產權，■一年□二年後可公開查詢

執行單位：修平技術學院

中　華　民　國　95　年　10　月　20　日

行政院國家科學委員會專題研究計畫成果報告

鑭錳氧化物/(絕緣氧化物,導體)異質微粒複合物中晶界自旋極化穿隧效應與磁傳輸機制的探討

Comparative study of the grain boundary tunnel-type magnetoresistance mechanism in the magnetic granular solid and thin film

計畫編號：NSC 94-2112-M-164-001-
執行期限：94 年 8 月 1 日至 95 年 7 月 31 日
主持人：楊尚霖教授兼系主任　　修平技術學院電機工程系
計畫參與人員：謝承達，林宸澂，林昆鴻，施旻吾

1. Abstract

本研究使用化學及固態燒結法製作 $(La_{0.7}Pb_{0.3}MnO_3)_{1-x}Ag_x$ 及 $(La_{0.7}Pb_{0.3}MnO_3)_{1-x}(Fe_2O_3)_x$ 陶瓷複合物。計畫中針對樣品的結構及磁傳輸將作詳細的研究。在兩系統中磁化率皆隨 Ag 或 Fe_2O_3 含量的增加而降低，而電阻係數在 $(La_{0.7}Pb_{0.3}MnO_3)_{1-x}Ag_x$ 中會明顯降低，$(La_{0.7}Pb_{0.3}MnO_3)_{1-x}(Fe_2O_3)_x$ 則急劇增加。主要乃是 Ag 進入晶界區域形成導電網路改善載子的傳輸。相反地，Fe_2O_3 在複合物樣品中在兩晶粒間充當一個分離層形成人工的穿透接面。在研究中觀察到加入 Ag 或 Fe_2O_3 皆會增加磁阻。本研究結果已發表於 SCI 期刊 ***Maternals Letter, Vol. 40, pp. 1682-1686***。對於晶界及其複合物的磁電特性已陸續完成投稿業經審查中。

關鍵字：鈣鈦礦，磁阻，電阻係數，晶界。

Ceramic composites of $(La_{0.7}Pb_{0.3}MnO_3)_{1-x}Ag_x$ and $(La_{0.7}Pb_{0.3}MnO_3)_{1-x}(Fe_2O_{3)x}$ are prepared by using chemical and solid-sate sintering route. The structural and magnetotransport properties are studied for these composites. Ferromagnetism is gradually suppressed with the increase of Ag or Fe_2O_3 mole percentage for both systems. The resistivity decreases significantly for $(La_{0.7}Pb_{0.3}MnO_3)_{1-x}Ag_x$ while resistivity increases dramatically for $(La_{0.7}Pb_{0.3}MnO_3)_{1-x}(Fe_2O_{3)x}$. It is suggested that the introduction of Ag into the niche of grain boundaries form artificial conducting network and improve the carriers to transport. Contrarily, the Fe_2O_3 in $(La_{0.7}Pb_{0.3}MnO_3)_{1-x}(Fe_2O_{3)x}$ composite acts as a separation layer between two grains and forms the artificial tunneling junction. However, the enhancement of magnetoresistance has been observed for both systems.

Keywords：Composite materials; Magnetic materials; Electrical Properties.

2. Introduction

Mixed-valence rare-earth manganese oxides, $Ln_{1-x}A_xMnO_3$ (where Ln=La, Nd, Pr, etc. and A=Ca, Sr, Ba, Pb, etc.), have recently been the materials of extensive research because of the rich variety of

crystallographic, magnetic and electronic phases [1-10]. These materials exhibit a large magnetoresistance ratio (MR ratio, defined as $[\rho(H)-\rho(0)]/\rho(H)$), termed as colossal magnetoresistance, which is greatly useful for various industrial applications. However, this property has been difficult to utilize for technological applications due to the large magnetic field of the order of several teslas required to obtain this effect. For most room temperature applications one needs an MR at low values of field. Thus, the important issues are to achieve a higher MR ratio at a lower applied field for these CMR compounds. Recently, the discovery that grain boundaries and interfaces can be important sources of low-field MR has attracted renewed interest in these polycrystalline compounds. Some attempts [11-13] have been observed the enhancement of MR ratio through the composites of $La_{1-x}Sr_xMnO_3/CeO_2$, $La_{1-x}Sr_xMnO_3$/silica, $La_{1-x}Ca_xMnO_3/SrTiO_3$, and $La_{1-x}Sr_xMnO_3$/glass. This enhancement can be explained by the model of spin-polarized tunneling with insulator layer as a barrier. However, the metal-insulator transition temperature also decreases with the increase of MR ratio. In this article, we intend to study the difference of magnetic and electrical properties between $(La_{0.7}Pb_{0.3}MnO_3)_{1-x}Ag_x$ (LPMO/Ag) and $(La_{0.7}Pb_{0.3}MnO_3)_{1-x}(Fe_2O_{3)x}$ (LPMO/FO) composites. The variation of magnetotransport behaviors between conductor-combined and insulator-combined composites will be discussed.

3. Experimental

The $(La_{0.7}Pb_{0.3}MnO_3)_{1-x}Ag_x$ and $(La_{0.7}Pb_{0.3}\ MnO_3)_{1-x}(Fe_2O_3)_x$ $(0 \leqq x \leqq 0.2)$ composites were prepared by two steps. First, the powder of pure $La_{0.7}Pb_{0.3}MnO_3$ was prepared by the conventional ceramic fabrication technique of solid-state reaction. After wet-milled by SPEX 8000M, well-dried hyperfine powders, La_2O_3 (99.95% purity), $PbCO_3$ (99.99% purity) and $MnCO_3$ (99.99% purity), were mixed by Retsch-Mix Miller MM-2000 in a stoichiometric ratio and calcined in air at 850^oC for 24 hours with intermediate grindings three times. Second, the combined powders of LPMO/Ag and LPMO/FO with stoichiometric ratios were mixed after grinding and then pressed into a disk-shape pellet with a diameter of 12 mm and a thickness of 2 mm. The disk samples were sintered in air at 750^oC for an hours and then cooled down to room temperature at a cooling rate of 3^oC/min. X-ray diffractograms were recorded with a powder diffractometer (Rigaku, PC-2000, Cu-K α radiation) at room temperature. The structure and phase purity of the samples were examined by the diffraction patterns recorded in the 2θ ranges from 20^o to 60^o. The scanning electron microscopy (SEM, Hitachi S-3000N) with energy dispersive x-ray analysis (EDX, Horoba Model 7021-H) were utilized to check the microstructure and composition. The magnetization measurements between 5 K and 350 K were performed in a Quantum Design superconducting quantum interference device MPMS-5S SQUID magnetometer.

The zero-field cooling (ZFC) and field cooling (FC) curves were taken in an applied field of 100 Oe. Temperature dependence of magnetization curves in an applied field of 50 kOe and field dependence of magnetization loops were also recorded at 5 K from -50 kOe to 50 kOe. Resistivity was obtained from the standard four-point probe method on bars of typical dimensions 10mm×1.5mm×1mm. The temperature dependence of resistivity measurements were collected with or without a field of 10 kOe parallel to the direction of electrical current between 5K and 350K.

4. Results and Discussion

Figure 1 shows the XRD patterns of LPMO/Ag and LPMO/FO samples indicating that the pure LPMO/Ag and LPMO/FO combined composites have been synthesized. The XRD spectra of the LPMO/Ag combined samples as shown in Fig. 1(a) shows two different sets of XRD peaks, which is corresponded a rhombohedra perovskite for $La_{0.7}Pb_{0.3}MnO_3$ and a cubic structure for Ag. No extra phase is obtained indicating that the reactions between the $La_{0.7}Pb_{0.3}MnO_3$ and Ag grain boundaries are negligible. In fact, XRD spectra show that the perovskite phase has already formed for the $La_{0.7}Pb_{0.3}MnO_3$ sample after calcination process. Hence, in the second step of combined sample synthesis, the sintering process could improve the crystallization and the shorter sintering time could decrease the inter-diffusion between $La_{0.7}Pb_{0.3}MnO_3$ and Ag grains. For the LPMO/FO composites as shown in Fig. 1(b), similar result is also observed.

To confirm the microstructure of the composites, we had imaged the samples with SEM. The micrographs as shown in Fig. 2 showing the surface morphology of x=0.2 for LPMO/Ag and LPMO/FO composites are selected presence. Two kinds of particles can be observed from the SEM images of the both composite systems. For LPMO/Ag system, square area (1μm×1μm) EDX profile shown in Fig. 3(a) clearly confirms that they consist almost entirely of Ag for spectrum 1 in Fig. 2(a). The presence of C element in the all EDX profiles is due to the carbon paint for sample mounting. On other hand, the regions away from spectrum 1 show the composition of $La_{0.7}Pb_{0.3}MnO_3$ with no Ag content and EDX profile in Fig. 3(b) of spectrum 2 is selected for presence. Similarly, the EDX profiles of spectrum 3 and spectrum 4 in Fig. 2(b) of LPMO/FO (x=0.2) composite are shown in Fig. 4. The present results demonstrate that the samples of both composite systems indeed consist of LPMO/Ag and LPMO/FO combined phases

The ZFC and FC magnetization curves as shown in Fig. 5 are measured to exam the magnetic behavior in a low field of 100 Oe for both of the composite systems. For x = 0 compounds of both systems, the ZFC and FC magnetization curves, except at very low temperature, are almost overlap indicating a ferromagnetic state. Conversely, in the Ag and Fe_2O_3 combined compounds, the ZFC curves coincide with the FC curves at high temperature, but separate as temperature

decreasing below the ferromagnetic transition temperature T_C (defined as the temperature where the slope, $|dM/dT|$, reaches a maximum value calculated from the ZFC curve) showing a λ-shape curve. The irreversibility is found for Ag and Fe_2O_3 combined composites, and indicates the existence of ferromagnetic cluster. It is reasonable that the Mn-Mn magnetic exchange would be interrupted, and conquently, Mn spin disorders would occur at the interfaces due to $La_{0.7}Pb_{0.3}MnO_3$ grains are partly separated by Ag or Fe_2O_3. As Fig 5(a) and 5(b) show, the unchanged T_C (around 350K) indicates no variation in Mn^{4+} and oxygen content due to low temperature sintering.

Figure 6 shows the temperature dependence of magnetization curves in an applied field of 50 kOe for the LPMO/Ag and LPMO/FO composites. The samples undergo a paramagnetic to ferromagnetic transition with the decrease of temperature. For both of the two systems, the saturation magnetization (M_S, defined as the magnetization at 5 K and an applied field of 50 kOe for comparison) decreases with the increase of Ag or Fe_2O_3 content. The addition of Ag or Fe_2O_3 does not change the magnetic transition of $La_{0.7}Pb_{0.3}MnO_3$, but leads to a decrease in M_S due to the magnetic dilution. M_S decreases with increasing x as would be expected due to the decrease in content fraction of $La_{0.7}Pb_{0.3}MnO_3$ phase and increase of non-ferromagnetic materials. It is seen that the decrease of M_S with increasing x for LPMO/FO system is larger than that of LPMO/Ag system. It is for the reason that the volume percent of Fe_2O_3 is larger than that of Ag with the same x (mole content).

The field dependence of magnetization curves recorded at 5 K from -50 kOe to 50 kOe for the LPMO/Ag and LPMO/FO composites are shown as Fig. 7. All of the composites show relatively square loops indicating the similar magnetization process. The values of saturation magnetization M_S, obtained from the hysteresis curves at 5 K and 50 kOe, decrease with the increase of Ag or Fe_2O_3 content. These results are consistent with the data of high-field magnetization in Fig. 6.

Figure 8 shows the temperature dependence of resistivity and MR ratio obtained under the applied magnetic fields of 0 Oe or 10 kOe for pure $La_{0.7}Pb_{0.3}MnO_3$, $(La_{0.7}Pb_{0.3}MnO_3)_{0.8}Ag_{0.2}$ and $(La_{0.7}Pb_{0.3}MnO_3)_{0.8}(Fe_2O_3)_{0.2}$ composites. It is found that the presence of Ag in $La_{0.7}Pb_{0.3}MnO_3$ matrices results in a decrease of resistivity and a lowering of the metal-insulator transition temperature. The decrease of resistivity can be explained by the formation of conduction channels by Ag among $La_{0.7}Pb_{0.3}MnO_3$ grains. Conversely, the increase of resistivity is observed with the addition of Fe_2O_3 in $La_{0.7}Pb_{0.3}MnO_3$ grain matrices. This result is obviously attributed to the spin-polarized electron tunneling with grain boundaries as the barriers. Thus, the electron hopping across the insulating coupling layers, Fe_2O_3, meets high resistance at zero-field. With an external field applied of 10 kOe, resistivity

decreases due to the suppression of spin scattering and enhanced MR ratio is obtained. Thus, the MR ratio of $(La_{0.7}Pb_{0.3}Mn\ O_3)_{0.8}(Fe_2O_3)_{0.2}$ composite is larger than that of $(La_{0.7}Pb_{0.3}MnO_3)_{0.8}Ag_{0.2}$ composite.

5. Conclusion

In summary, ceramic composites of LPMO/Ag and LPMO/FO are synthesized by using the chemical solid-state method. These composites were characterized for their structural, magnetic and transport properties. Ferromagnetism is suppressed due to the magnetic dilution. Magnetoresistance ratio increases with the Ag and Fe_2O_3 combined composites. The results of this study demonstrate that the magnetoresistive sensitivity can be enhanced by utilizing the LPMO/Ag and LPMO/FO composites. This work was sponsored by the National Science Council of the Republic of China under the grant No. NSC94-2112-M-164-001.

References

1. R.-M. Thomas, V. Skumryev, J.M.D. Coey and S. Wirth, J. Appl. Phys. 85 (1999) 5384.
2. B. X. Gu, S. Y. Zhang, H. C. Zhang and B. G. Shen, J. Mag. Mag. Mater. 204 (1999) 45.
3. K. Ghosh, S. B. Ogale, R. Ramesh, R. L. Greene, T. Venkatesan, K. M. Gapshup, R. S. Bathe and S. I. Patil, Phys. Rev. B 59 (1999) 533
4. J.J. Neumeier and J.L. Cohn, Physi. Rev. B 61 (2000) 14319.
5. S. Roy and N. Ali, J. Appl. Phys. 89 (2001) 7425.
6. C. Mitra, P. Raychaudhuri, J. John, S.K. Dhar, A.K. Nigam and R. Pinto, J. Appl. Phys. 89 (2001) 524.
7. S.L. Young, Y.C. Chen, H.Z. Chen, L. Horng and J.F. Hsueh, J. Appl. Phys. 91 (2002) 8915.
8. N. Shannon and A.V. Chubukov, Phys. Rev. B 65 (2002) 104418.
9. G.T. Tan, S. Dai, P. Duan, Y.L. Zhou, H.B. Lu and Z.H. Chen, Phys. Rev. B 68 (2003) 014426.
10. S. Zhang, L. Luan, S. Tan and Y. Zhang, Phys. Rev. Lett. 84 (2004) 3100.
11. D.K. Petrov, L. Krusin-Elbaum, J.Z. Sun, C. Feild, and P.R. Duncombe, Appl. Phys. Lett. 75 (1999) 995.
12. Ll. Balcells, A. E. Carrillo, B. Martínez, and J. Fontcuberta, Appl. Phys. Lett. 74 (1999) 4014.
13. S. Gupta, R. Ranjit, C. Mitra, P. Raychaudhuri and R. Pinto, Appl. Phys. Lett. 78 (2001) 362.

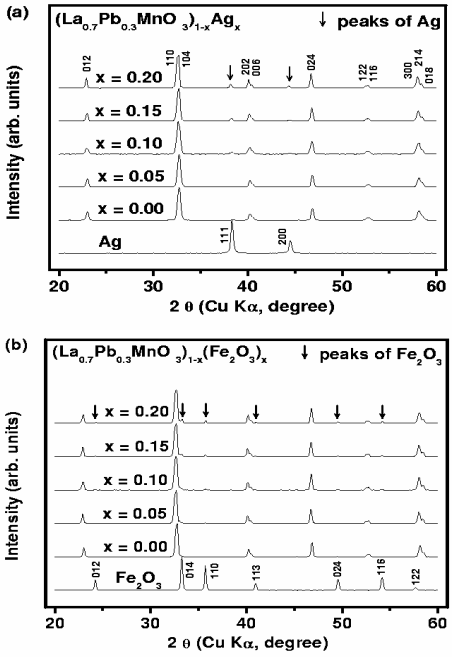

Fig. 1 X-ray diffractograms for the (a)LPMO/Ag and (b)LPMO/FO composites.

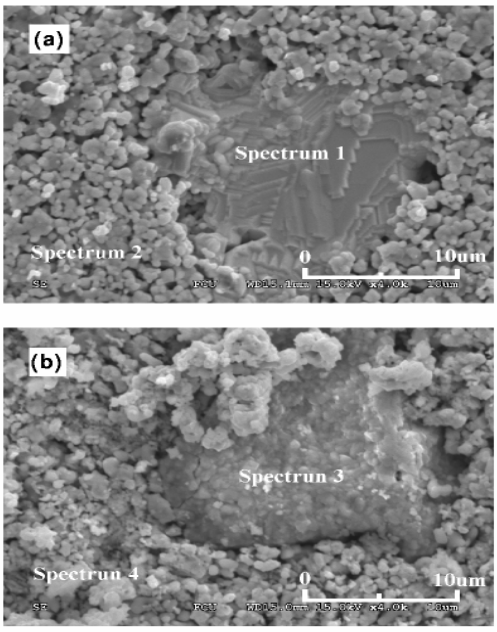

Fig. 2. The micrographs showing the surface morphology of x=0.2 for (a) LPMO/Ag and (b) LPMO/FO composites.

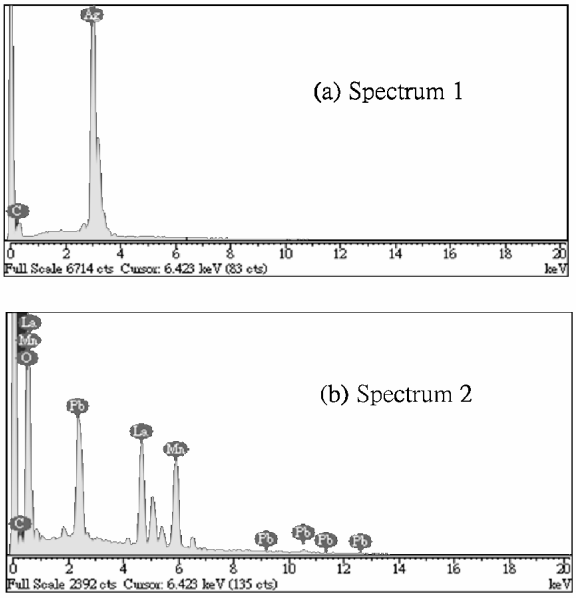

Fig. 3. EDX profiles of spectrum 1 and spectrum 2 shown in Fig. 3(a).

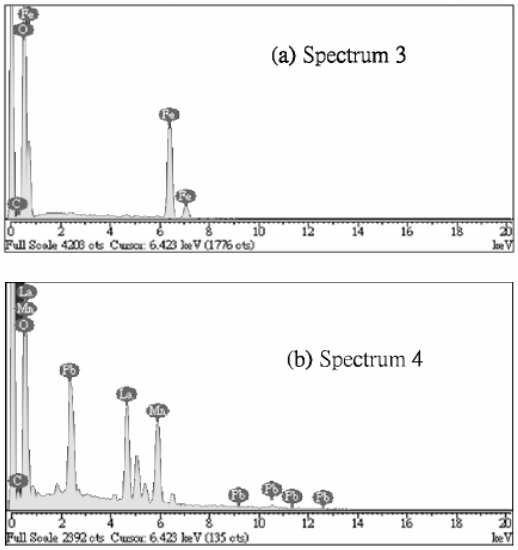

Fig. 4. EDX profiles of spectrum 3 and spectrum 4 shown in Fig. 3(b)

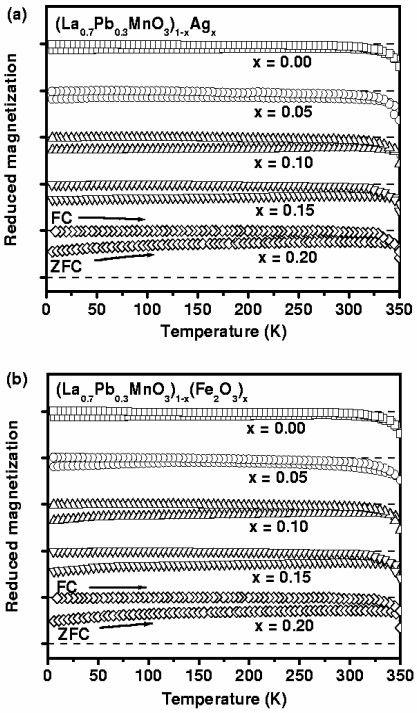

Fig. 5. Temperature dependence of ZFC and FC magnetization curves at an applied field of 100 Oe for the (a)LPMO/Ag and (b)LPMO/FO composites.

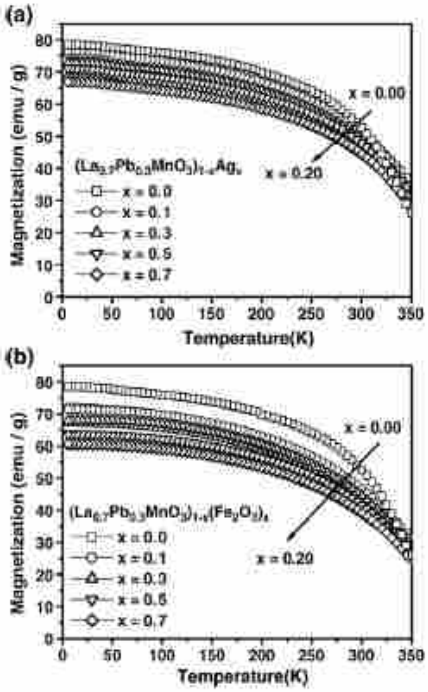

Fig. 6. Temperature dependence of magnetization curves in an applied field of 50 kOe for the (a) LPMO/Ag and (b) LPMO/FO composites.

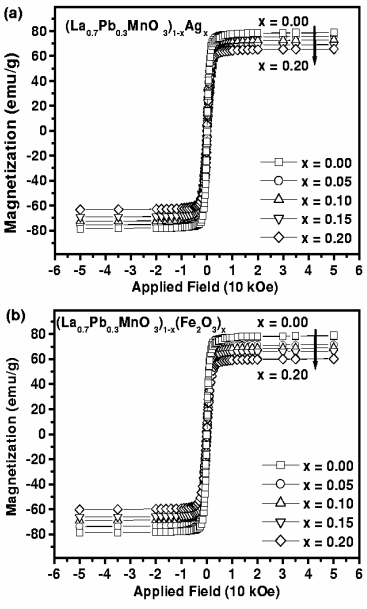

Fig. 7. Field dependence of magnetization curves recorded at 5 K from -50 kOe to 50 kOe for the (a)LPMO/Ag and (b)LPMO/FO composites

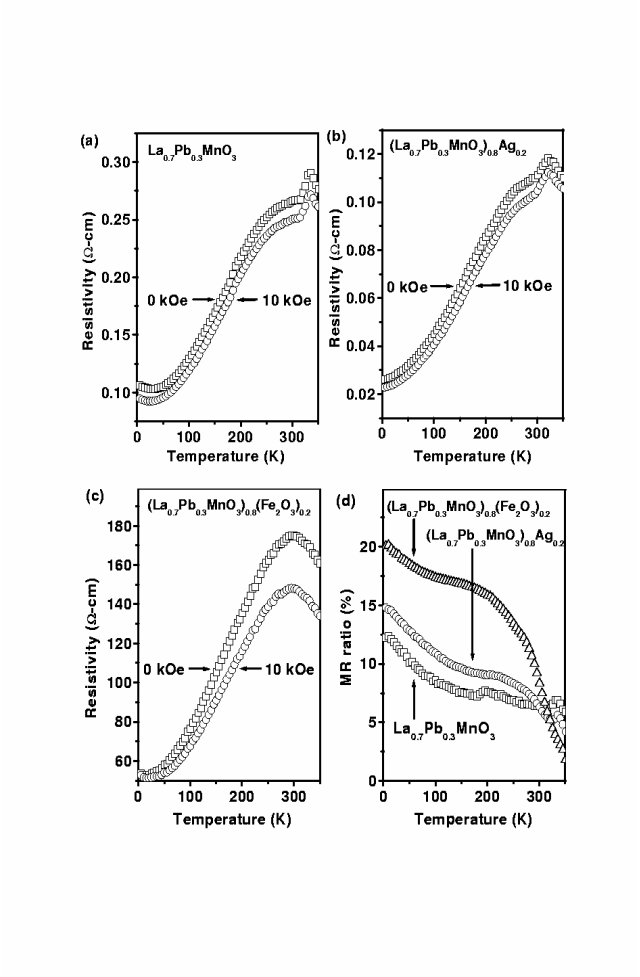

Fig. 8. Temperature dependence of resistivity for (a) pure $La_{0.7}Pb_{0.3}MnO_3$, (b) $(La_{0.7}Pb_{0.3}MnO_3)_{0.8}Ag_{0.2}$ and (c) $(La_{0.7}Pb_{0.3}MnO_3)_{0.8}(Fe_2O_3)_{0.2}$ composites. (d) Temperature dependence of MR ratio for pure $La_{0.7}Pb_{0.3}MnO_3$, $(La_{0.7}Pb_{0.3}MnO_3)_{0.8}Ag_{0.2}$ and $(La_{0.7}Pb_{0.3}Mn\ O_3)_{0.8}(Fe_2O_3)_{0.2}$ composites.